ARTICLE

BRD4 regulates PAI-1 expression in tumor-associated macrophages to drive chemoresistance in colorectal cancer

Dun Pan[1,2,3,7], Jinfeng Hu[1,7], Guo Li[1,7], Xuming Gao[1], Jie Wang[1], Leisi Jiang[1], Hong Lin[1], Yulin Chen[1], Yanheng Chen[3], Yiran Zheng[3], Junjin Lin[4], Min Zheng[1], Hui Chen[2]✉, Lin-Feng Chen[3,5,6]✉ and Xiangming Hu[1]✉

Tumor-associated macrophages (TAMs) in the tumor microenvironment play a key role in drug resistance, but the mechanisms underlying TAM polarization and its role in drug resistance remain unclear. Here, we identified BRD4 as a critical factor in TAM polarization and drug resistance in colorectal cancer (CRC). BRD4 deficiency in macrophages impaired M2-like TAM polarization, and tumors from myeloid-lineage specific *Brd4* conditional knockout (*Brd4*-CKO) mice displayed a reduction in infiltrating M2-like TAMs and an enhanced anti-tumor microenvironment. Colon cancer cells treated with conditioned medium from polarized *Brd4*-deficient TAMs, as well as tumors in *Brd4*-CKO mice, were more sensitive to oxaliplatin. RNA-seq and cytokine microarray analysis revealed that mRNA and protein levels of PAI-1 were significantly decreased in *Brd4*-deficient polarized TAMs. BRD4 was recruited to the promoter of *Serpine1*, promoting SMAD-dependent PAI-1 expression. Supplementing *Brd4*-deficient TAMs with recombinant PAI-1 hampered the sensitivity of colon cancer cells to oxaliplatin. Moreover, PAI-1 inhibitor and oxaliplatin synergistically suppressed the growth of colon tumors. Clinically, the expression levels of BRD4 in TAMs and PAI-1 in tumors were elevated in CRC patients with chemoresistance, correlating with shorter recurrence-free survival. Collectively, our findings uncover a novel role for BRD4 in TAM polarization and drug resistance via PAI-1 upregulation, suggesting the BRD4/PAI-1 axis as a potential prognostic marker and therapeutic target in CRC.

Oncogene; https://doi.org/10.1038/s41388-025-03453-6

INTRODUCTION

Colorectal cancer (CRC) is the third most common cancer and the second leading cause of cancer-related deaths, with around 2 million new cases and over 900,000 deaths annually [1]. While the targeted therapies and immune checkpoint blockade (ICB) therapy are able to extend the overall survival in some patients, chemotherapy is still the most common and effective treatment for those with advanced or unresectable tumors [2–4]. However, resistance to chemotherapy, including both intrinsic and acquired resistance, frequently arises during treatment, leading to therapeutic failure [5]. It is urgently needed to understand the mechanisms for drug resistance to facilitate the development of new therapeutic avenues with better clinical outcomes in CRC.

Tumor cell heterogeneity and the immunosuppressive tumor microenvironment (TME) are the two major contributing factors in drug resistance [6]. TME is composed of various components, including immune cells, fibroblasts, blood vessels, extracellular matrix, and regulatory proteins [7]. Tumor-associated macrophages (TAMs) are the most abundant immune cells within TME and predominantly exist as two distinct, polarized subtypes: M1-like TAMs and M2-like TAMs. M1-like TAMs, which are pro-inflammatory and anti-tumor, are prevalent during the early stages of tumor development, whereas M2-like TAMs, which are pro-tumor, emerge in the intermediate and late stages. These M2-like TAMs facilitate cancer cell survival, progression, invasion, metastasis, angiogenesis, and drug resistance by mediating immunosuppressive signaling [8–10]. For example, M2-like macrophages could produce surface proteins, such as PD-L1 and IL-10, to impede the functionality of effector T cells or release soluble factors that recruit the regulatory T cells, for cancer cell proliferation and progression [11, 12]. At the same time, the soluble factors from TAMs could directly target tumor cells, activating various pro-survival signaling pathways to inhibit cell apoptosis and promote the chemoresistance [10–12]. However, how the expression of these pro-survival factors from TAMs of CRC that contribute to chemoresistance is regulated remains to be further elucidated.

Plasminogen activator inhibitor-1 (PAI-1), encoded by the *SERPINE1* gene, regulates plasminogen activation and fibrinolysis [13]. Beyond these roles, PAI-1 promotes tumorigenesis by enhancing cancer cell proliferation, invasion, metastasis, and angiogenesis [14]. Elevated expression of PAI-1 is observed in various cancer types, including CRC, and its high levels are associated with poor prognosis and drug resistance, likely through

[1]Fujian Key Laboratory of Translational Research in Cancer and Neurodegenerative Diseases, Institute for Basic Medical Sciences, School of Basic Medical Sciences, Fujian Medical University, Fuzhou, China. [2]Department of Gastrointestinal Surgery, The First Affiliated Hospital of Fujian Medical University, Fuzhou, China. [3]Department of Biochemistry, College of Liberal Arts & Sciences, University of Illinois at Urbana-Champaign, Urbana, IL, USA. [4]Public Technology Service Center, Fujian Medical University, Fuzhou, China. [5]Carl R. Woese Institute for Genomic Biology, University of Illinois at Urbana-Champaign, Urbana, IL, USA. [6]Cancer Center at Illinois, University of Illinois Urbana-Champaign, Urbana, IL 61801, USA. [7]These authors contributed equally: Dun Pan, Jinfeng Hu, Guo Li. ✉email: chenhui@fjmu.edu.cn; lfchen@illinois.edu; xmhu2003@fjmu.edu.cn

Received: 10 January 2025 Revised: 5 May 2025 Accepted: 15 May 2025
Published online: 28 May 2025

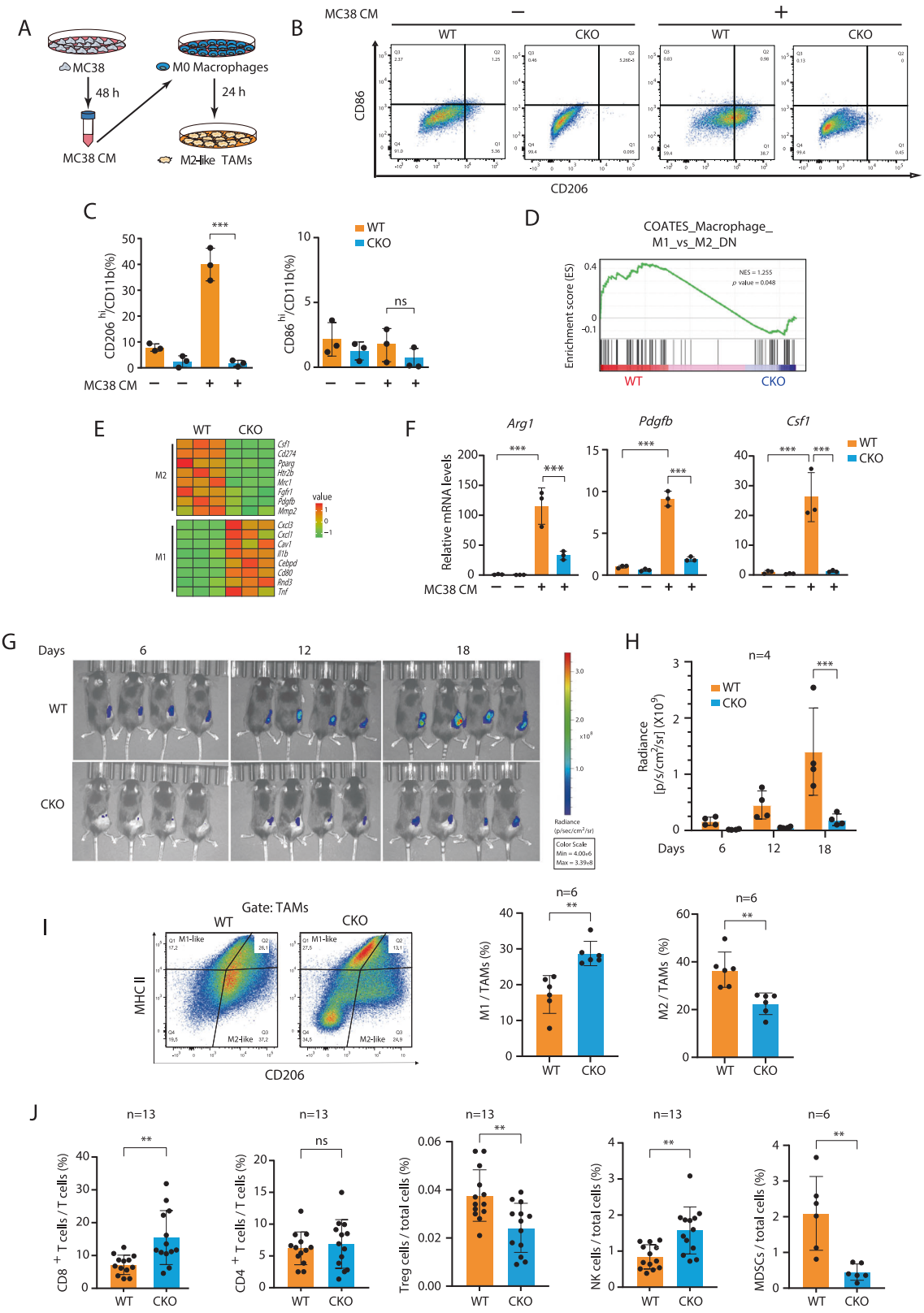

the inhibition of cell apoptosis and autophagy [15, 16]. For instance, elevated PAI-1 expression reduces the responsiveness of CRC patients to radiotherapy and chemotherapy [16]. PAI-1 expression in cancer cells is regulated by various factors, including growth factors, hormones, and proinflammatory cytokines, either directly or indirectly [14, 16]. TGF-β-mediated SMAD signaling has been identified as a major driver of PAI-1 expression in cancer cells [17]. TGF-β induces the binding of SMAD3 and SMAD4 to the CAGA boxes in the *SERPINE1* promoter, thereby promoting PAI-1 expression [17]. Furthermore, TGF-β also facilitates the interaction

Fig. 1 BRD4 regulates the polarization of TAMs and the immunosuppressive TME. A Experimental schematic for in vitro polarization of bone marrow-derived macrophages (BMDMs) into M2-like tumor-associated macrophages (TAMs) via treatment with MC38 conditioned medium (CM) for 24 h. **B** WT and *Brd4*-deficient BMDMs were polarized as described in (**A**) and analyzed for CD86 and CD206 expression on $CD11b^+$ cells using flow cytometry. **C** Quantification of $CD206^{hi}$ and $CD86^{hi}$ cells within the $CD11b^+$ TAM population ($n = 3$). **D** Gene Set Enrichment Analysis (GSEA) plot for COATES_Macrophage_M1_vs _M2_DN in polarized WT and *Brd4*-deficient TAMs, based on RNA sequencing (RNA-seq) data. **E** Heatmap illustrating the expression levels of M1- and M2-associated genes in polarized WT and *Brd4*-deficient TAMs, as determined by RNA-seq. **F** qRT-PCR analysis of mRNA expression levels of *Arg1*, *Pdgfb*, and *Csf1* in polarized WT and *Brd4*-deficient TAMs ($n = 3$). MC38-Luc cells were inoculated subcutaneously into the right flank of WT or *Brd4*-CKO mice. Tumor growth was monitored using bioluminescence imaging (**G**) with quantification of tumor size (**H**) ($n = 4$) at the indicated time points. **I** Left panel: Tumors from MC38-inoculated WT and *Brd4*-CKO mice were harvested on day 19. The expression of markers for M1-like TAMs (MHCII high, CD206 low) and M2-like TAMs (MHCII low, CD206 high) was assessed in the total TAM population ($CD45^+CD11b^+F4/80^+Gr1^-$). Right panel: Proportion of M1-like and M2-like TAMs within the total TAM population ($n = 6$). **J** Percentage of various immune cell types (T cells and NK cells, $n = 13$; MDSCs, $n = 6$) in tumors from WT and *Brd4*-CKO mice. Data are presented as mean ± SD. Statistical significance was assessed using a two-tailed Student's *t* test for comparisons between two groups and two-way ANOVA with Tukey's post-hoc test for multiple comparisons. $^*p < 0.05$, $^{**}p < 0.01$, $^{***}p < 0.001$. ns not significant.

between SMADs and other transcription factors, such as Sp1, to regulate PAI-1 expression in cancer cells [18]. In addition to cancer cells, other cells within the TME, including TAMs, could also produce PAI-1 through paracrine or autocrine mechanisms [19, 20]. However, the mechanisms underlying PAI-1 regulation in these non-cancerous cells, particularly TAMs, remain poorly understood.

Bromodomain-containing factor BRD4 plays a crucial role in the epigenetic regulation of gene expression in both inflammation and cancer via binding to acetylated histones or non-histone proteins through its two bromodomains [21]. Studies using myeloid-specific *Brd4* conditional knockout mice demonstrate that BRD4 regulates the protective and pathogenic functions of macrophages by controlling distinct genes expression in cooperation with various transcription factors [22–24]. For example, BRD4 regulated NF-kB-dependent inflammatory gene expression in macrophages during LPS-induced sepsis [22]. It also cooperated with IRF8 to activate NLRC4 inflammasome, promoting the production of IL-1b and IL-18 in response to *Salmonella* infection [23]. Additionally, BRD4 regulated M1 macrophage activation and HIF-1α-dependent glycolysis for the clearance of *H. pylori* infection [24]. While these studies underscore the pivotal role of BRD4 in innate immunity by modulating inflammatory gene expression in macrophages, its potential role in the polarization of TAMs in cancer remains to be fully elucidated.

Here, we demonstrate that BRD4 regulates the polarization of M2-like TAMs both in vitro and in vivo. BRD4 facilitates SMADs-mediated transcription of *Serpine1* and the subsequent production of PAI-1 in M2-like TAMs, thereby contributing to resistance to oxaliplatin in CRC. These findings uncover a novel regulatory role of BRD4 in TAMs, highlighting its ability to modulate TME and influence drug resistance in cancer.

RESULTS

BRD4 regulates the polarization of M2-like TAMs and TME

To explore the potential role of BRD4 in the polarization of TAMs, we treated wild-type (WT) or *Brd4*-deficient bone marrow-derived macrophages (BMDMs) with conditioned media (CM) of MC38 murine colon adenocarcinoma cells, which polarize BMDMs to M2-like TAMs [25, 26] (Fig. 1A). When WT BMDMs were treated with CM of MC38, a significant number of macrophages ($CD11b^+$) expressed CD206, a M2-like TAM marker (Fig. 1B, C) while very limited number of cells expressed CD86, a M1-like TAM marker (Fig. 1B, C). However, the population of $CD206^+$ macrophages was not enhanced by CM in *Brd4*-deficient BMDMs (Fig. 1B, C). Gene set enrichment analysis of the transcriptome data showed reduced expression of M2-associated gene sets in polarized *Brd4*-deficient TAMs compared to WT TAMs, indicating impaired M2-like TAM polarization (Fig. 1D). RNA sequencing heatmap further confirmed significant downregulation of M2-associated genes and upregulation of M1-associated genes in polarized *Brd4*-deficient TAMs (Fig. 1E). Quantitative RT-PCR corroborated these findings, demonstrating decreased expression of key M2-like TAM markers, including *Arg1*, *Pdgfb*, and *Csf1* [27, 28], in polarized *Brd4*-deficient TAMs (Fig. 1F). These findings underscore the crucial role of BRD4 in the polarization of M2-like TAMs.

To evaluate the role of BRD4 in the polarization of TAMs in vivo, we employed the MC38 syngeneic subcutaneous CRC mouse model [29], in which MC38-Luc cells (MC38 cells stably expressing firefly luciferase) were injected subcutaneously into WT or *Brd4*-CKO mice. Tumors grew in WT mice in a time-dependent manner as visualized by the IVIS® Spectrum In Vivo Imaging System (Fig. 1G, H). However, tumors from *Brd4*-CKO mice were much smaller than those in WT mice, indicating that deletion of *Brd4* in myeloid cells suppresses tumor formation. Consistent with a tumor-promoting role of M2-like TAMs, we found that tumors from *Brd4*-CKO mice constituted decreased M2-like ($MHCII^{low}CD206^{high}$) but increased M1 ($MHCII^{high}CD206^{low}$) TAMs (Fig. 1I). These data demonstrate that BRD4 regulates the polarization of M2-like TAMs and tumor growth in vivo.

Since TAMs are a major component of TME, contributing to the immunosuppressive environment by affecting the infiltration of various immune cells [30], the altered ratio of M1-like/M2-like TAMs in the *Brd4*-CKO mice (Fig. 1I) suggested that tumors from these mice might have a distinct TME. Indeed, comparing to WT mice, tumors from *Brd4*-CKO mice were associated with increased anti-tumor $CD8^+$ T cells and NK (nature killing) cells but reduced pro-tumor Tregs (regulatory T cells) and MDSCs (myeloid-derived suppressive cells) with no difference in the $CD4^+$ T cells (Fig. 1J & Supplementary Figs. S1–S4). All together, these data suggest that BRD4 not only regulates the polarization of M2-like TAMs, but also contributes to the immunosuppressive TME.

Tumor-bearing *Brd4*-CKO mice are more sensitive to oxaliplatin

The immunosuppressive TME contributes significantly to the resistance of cancer cells against therapies, including chemotherapy [31, 32]. TAMs are critical components of the TME and modulate drug resistance [31]. Since tumors from *Brd4*-CKO mice exhibited a reduced population of M2-like TAMs and a remodeled TME compared to their WT counterparts (Fig. 1), we hypothesized that these tumors would display altered sensitivities to chemotherapy. To test this, we evaluated the response of tumors from WT and *Brd4*-CKO mice to oxaliplatin, a widely used chemotherapeutic agent in CRC [33]. Upon injection of MC38 cells, tumors developed in WT mice (Fig. 2A). Oxaliplatin treatment, starting six days post-injection, significantly reduced tumor size and weight in WT mice (Fig. 2A–C). While tumors in *Brd4*-CKO mice were smaller than those in WT counterparts (Fig. 2A), oxaliplatin dramatically inhibited tumor growth in *Brd4*-CKO mice (Fig. 2A–C), indicating that BRD4 deficiency in myeloid cells enhances tumor sensitivity to the drug.

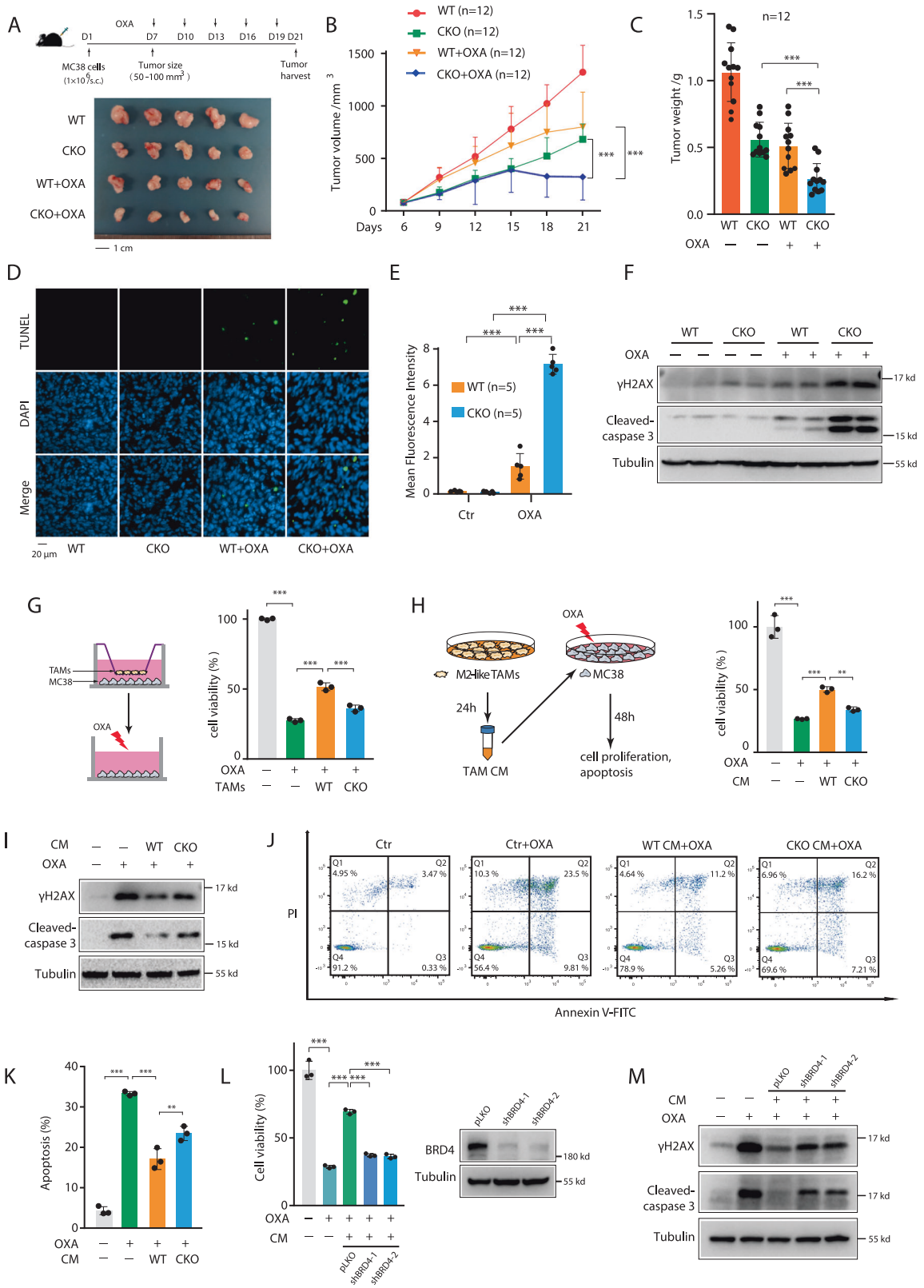

The cytotoxicity of oxaliplatin relies on its ability to induce DNA damage and apoptosis in cancer cells [34]. To assess the impact on DNA damage and apoptosis, we evaluated tumors from WT and *Brd4*-CKO mice with or without oxaliplatin treatment. Oxaliplatin increased γH2AX levels in tumors from WT mice, with higher levels observed in tumors from *Brd4*-CKO mice (Supplementary Fig. S5, Fig. 2F). There was barely any TUNEL staining in the tumors from either WT or *Brd4*-CKO mice (Fig. 2D, E), indicating that the reduced tumor growth in *Brd4*-CKO mice was unlikely due to increased cellular apoptosis. In contrast, oxaliplatin treatment

Fig. 2 Myeloid BRD4 deficiency enhances sensitivity of MC38 cells to oxaliplatin in vivo and in vitro. A Top: schematic of the experimental design. WT or *Brd4*-CKO mice were subcutaneously inoculated with MC38 cells. At day 7, mice with tumor volumes of 50–100 mm^3 received intraperitoneal injections of oxaliplatin (OXA) (6 mg/kg body weight) every 3 days. Tumors were harvested at day 21 for subsequent analysis. Bottom: Representative images of tumors from WT and *Brd4*-CKO mice with or without oxaliplatin treatment. Tumor volumes (**B**) and weights (**C**) from the experiments described in (**A**) were measured ($n = 12$). Representative images (**D**) and quantification (**E**) of TUNEL staining in tumor tissues from (**A**) ($n = 5$). **F** Immunoblot analysis of γH2AX and cleaved caspase 3 levels in tumor tissues from (**A**). Data represent results from two animals per group. **G** Polarized WT and *Brd4*-deficient TAMs on 0.4 μm transwell filters were co-cultured with MC38 cells for 24 h. After removal of TAMs, MC38 cells were treated with OXA (30 μM) for an additional 48 h. MC38 cell viability was assessed using the MTS assay ($n = 3$). **H** MC38 cells were treated with CM from polarized WT or *Brd4*-deficient TAMs for 4 h, followed by treatment with or without OXA (30 μM) for 48 h. MC38 cells were then analyzed for cell viability. **I** γH2AX and cleaved caspase 3 levels in MC38 cells from (**H**). **J**, **K** Flow cytometric analysis of apoptotic MC38 cells from (**H**), using Annexin V/PI staining. Representative FACS dot plots (**J**) and quantification of apoptotic cells (**K**) ($n = 3$). **L** HCT116 cells were treated with CM from polarized WT or BRD4 knockdown THP-1-derived TAMs for 4 h, followed by treatment with or without OXA (30 μM) for 48 h. Cell viability was measured by MTS assay, and BRD4 knockdown efficiency is shown on the right. **M** γH2AX and cleaved caspase 3 levels in HCT116 cells from (**L**). Data are expressed as mean ± SD. Statistical analyses were performed using two-way ANOVA with Tukey's post-hoc test for multiple comparisons. $^{**}p < 0.01$, $^{***}p < 0.001$.

significantly increased TUNEL staining in WT tumors (Fig. 2D, E), reflecting its cytotoxic effect. Notably, oxaliplatin treatment induced a marked increase in TUNEL staining in *Brd4*-CKO tumors (Fig. 2D, E), indicating that the absence of BRD4 in TAMs potentiates oxaliplatin-induced apoptosis. Correspondingly, caspase-3 activation was significantly enhanced in *Brd4*-CKO tumors following oxaliplatin treatment compared to WT tumors (Fig. 2F). These results demonstrate that BRD4 deficiency in myeloid cells sensitizes colon tumors to oxaliplatin by promoting apoptosis in tumor cells.

To determine whether the enhanced cytotoxicity of oxaliplatin in *Brd4*-CKO mice was directly mediated by TAMs, we employed a transwell co-culture system to separate polarized TAMs from MC38 cells (Fig. 2G). In this setup, soluble factors released from polarized TAMs were able to diffuse through the membrane and influence MC38 cells. We observed a significant increase in MC38 cell viability upon oxaliplatin treatment when cultured with polarized WT TAMs, compared to cultures without TAMs. In contrast, co-culture with polarized *Brd4*-deficient TAMs resulted in only a minimal increase in MC38 cell viability (Fig. 2G). To further elucidate the role of these soluble factors, we analyzed CM from polarized WT and *Brd4*-deficient TAMs. As expected, CM from WT TAMs enhanced MC38 cell viability with reduced DNA damage and apoptosis, while CM from *Brd4*-deficient TAMs had no effect (Fig. 2H–K). Similar results were also obtained using human cell lines. CM from THP-1-derived WT TAMs increased HCT116 cell viability with reduced DNA damage and apoptosis, while CM from THP-1-derived TAMs with *Brd4*-knockdown had no impact (Fig. 2L, M). These findings suggest that BRD4-regulated soluble factors secreted by TAMs, rather than direct cell contact, modulate the sensitivity of CRC cells to oxaliplatin.

BRD4 regulates PAI-1 expression in polarized M2-like TAMs

To identify the BRD4-regulated factor(s) in TAMs that affect the response of MC38 cells to oxaliplatin, we performed RNA sequencing (RNA-seq) analysis of MC38 CM polarized WT and *Brd4*-deficient TAMs. Given that BRD4 is an epigenetic regulator, it is likely to modulate the transcription of these unidentified factor(s). While BRD4 deficiency altered certain gene expression in unpolarized M0 macrophages, CM treatment significantly affected gene expression in polarized TAMs (Fig. 3A). In polarized WT TAMs, we identified 152 upregulated genes compared to their unpolarized counterparts, while 192 genes were downregulated in polarized *Brd4*-deficient TAMs relative to polarized WT TAMs. Notably, 105 genes overlapped as BRD4-regulated genes (Fig. 3B, C). Gene ontology (GO) enrichment analysis revealed that these genes were involved in regulating cellular immune responses, particularly innate immunity (Fig. 3D). Kyoto Encyclopedia of Genes and Genomes (KEGG) pathway analysis identified their role in immune signaling, including cytokine-cytokine receptor interaction and chemokine signaling (Fig. 3E). These findings suggest that BRD4 regulates the TAM-mediated immune response and modulates paracrine communication between TAMs and other cells within TME.

The ability of TAMs to affect MC38 cell response to oxaliplatin appears to be mediated by soluble factor(s) secreted from TAMs (Fig. 2). Therefore, we analyzed the secreted proteins in the CM of polarized WT and *Brd4*-deficient TAMs using Proteome Profiler Mouse Cytokine Array kit, which includes cytokines, chemokines, growth factors and signaling molecules (Fig. 3F). Of the 111 proteins tested, 14 were significantly downregulated in *Brd4*-deficient polarized TAMs (Fig. 3F, G). By overlaying the RNA-seq data with the cytokine array results, we identified three key BRD4-regulated factors in polarized TAMs: PAI-1, M-CSF, and CD40 (Fig. 3H). Recombinant PAI-1 added to CM from *Brd4*-deficient TAMs significantly reduced oxaliplatin-induced cytotoxicity in MC38 cells, whereas M-CSF and CD40 had no such effect (Supplementary Fig. S6). These findings suggest that BRD4 regulates oxaliplatin resistance in MC38 cells by modulating PAI-1 expression in TAMs.

BRD4 cooperates with SMAD3/4 to regulate PAI-1 expression in TAMs

To investigate the molecular mechanism by which BRD4 regulates PAI-1 expression in TAMs, we examined *Serpine1* induction (encoding PAI-1) in WT BMDMs and THP-1 cells following exposure to MC38 or HCT116 CM, respectively (Fig. 4A, Supplementary Fig. S7). This induction was significantly reduced in polarized *Brd4*-deficient or *Brd4*-knockdown TAMs (Fig. 4A, Supplementary Fig. S7). ELISA or immunoblot analyses confirmed that both extracellular and intracellular PAI-1 levels increased in polarized WT TAMs, whereas no such increase was observed in polarized *Brd4*-deficient or *Brd4*-knockdown TAMs (Fig. 4B, C, Supplementary Fig. S8). Additionally, tumor extracts from WT mice displayed significantly higher PAI-1 levels compared to those from *Brd4*-CKO mice, further highlighting the critical role of BRD4 in TAMs for regulating PAI-1 (Fig. 4D).

BRD4 interacts with various transcription factors to promote gene expression [21], and SMAD3 and SMAD4 are key transcription factors of PAI-1 [17, 35]. We hypothesized that BRD4 cooperates with these SMAD proteins to regulate PAI-1 expression in polarized TAMs. To test this, we utilized SIS3, a SMAD3 inhibitor [36], which suppressed MC38 CM-induced SMAD3 phosphorylation and subsequent *Serpine1* transcription, as well as PAI-1 protein levels (Fig. 4E, F). These results confirm the essential role of SMAD3 in regulating PAI-1 expression.

Next, we examined the interaction between BRD4 and SMAD3/4. Notably, SIS3 treatment inhibited both SMAD3 phosphorylation and its interaction with SMAD4 [36]. Upon MC38 CM stimulation, BRD4's binding to both SMAD3 and SMAD4 in BMDMs was significantly increased (Fig. 4G). However, SIS3 treatment reduced the BRD4-SMAD3 interaction and almost completely abolished the

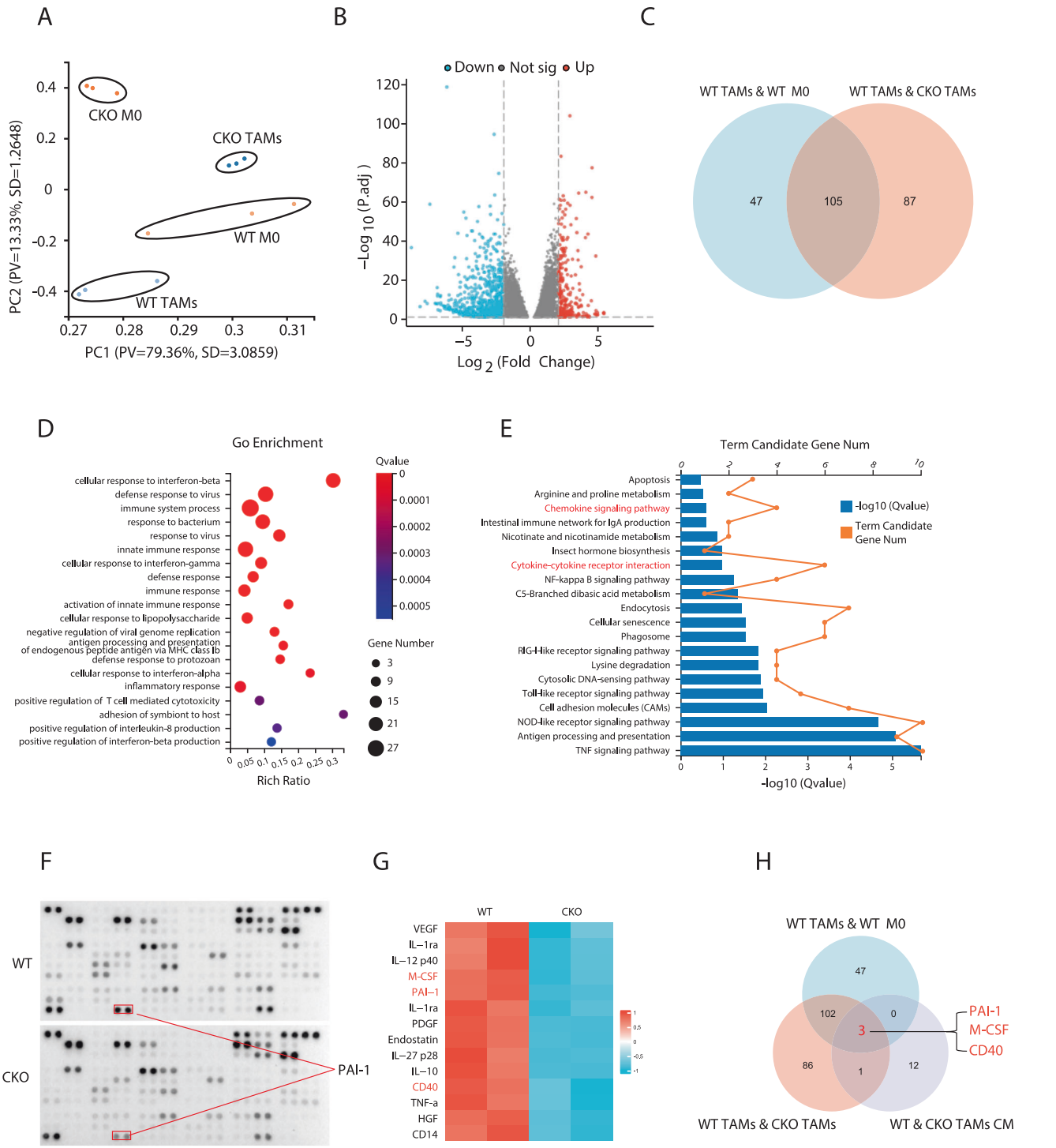

Fig. 3 Deletion of BRD4 alters the transcriptional landscape in TAMs. A Principal Component Analysis (PCA) of RNA-seq data from MC38 CM-polarized and unpolarized WT and *Brd4*-deficient TAMs. **B** Volcano plot of RNA-seq data comparing MC38 CM-polarized WT and *Brd4*-deficient TAMs. Upregulated genes in polarized *Brd4*-deficient TAMs relative to WT TAMs are indicated by red dots, downregulated genes by blue dots, and genes with no significant change by gray dots. **C** Venn diagram showing the number of genes with significantly altered expression (log2 fold change ≥2; FDR ≤ 0.05) in unpolarized or MC38 CM-polarized WT and *Brd4*-deficient TAMs. GO enrichment analysis (**D**) and KEGG pathway enrichment analysis (**E**) of the 105 overlapping genes from the Venn diagram in (**C**). **F** Proteome Profiler Mouse XL Cytokine Array analysis of supernatants from MC38 CM-polarized WT and *Brd4*-deficient TAMs. The position of PAI-1 is indicated in the representative images of the array results. **G** Heatmap of 14 proteins with reduced signals in polarized *Brd4*-deficient TAMs identified from (**F**), color-coded by Z-score. **H** Venn diagram showing the overlap of differentially expressed soluble proteins identified in (**F**) with differentially expressed genes from (**C**).

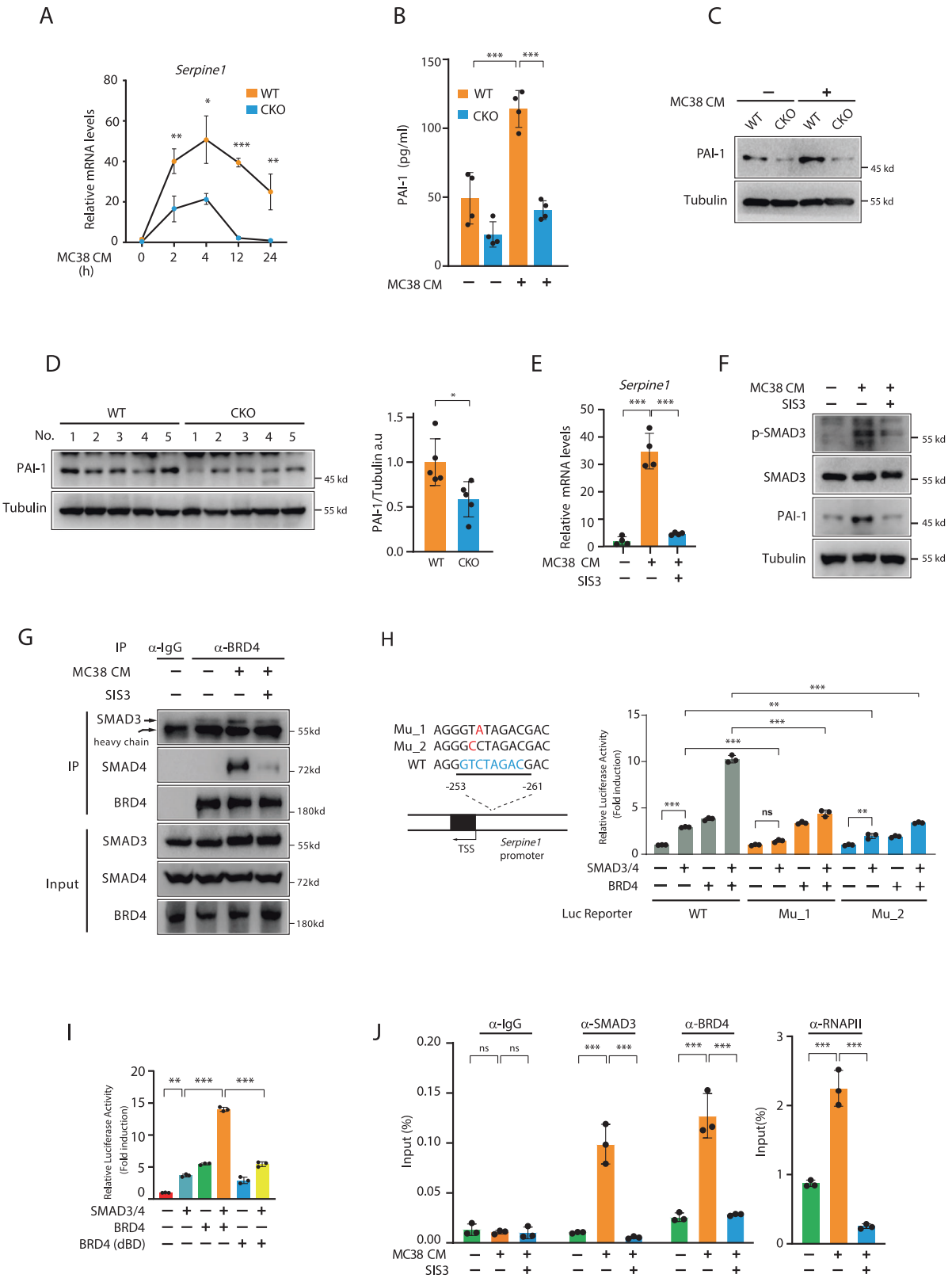

BRD4-SMAD4 interaction (Fig. 4G). These findings suggest that BRD4 interacts with SMAD3, and its interaction with SMAD4 is likely SMAD3-dependent.

A palindrome SMAD binding site was identified in the murine *Serpine1* promoter, located 253–261 bp upstream of the transcription start site [35] (Fig. 4H). To assess the cooperative activity of SMAD3 and BRD4, we cloned the *Serpine1* promoter into a luciferase reporter vector and co-transfected it with SMAD3 and SMAD4, as they work together to activate SMAD target genes [37]. While either SMAD3/SMAD4 or BRD4 alone moderately activated the reporter, their co-

Fig. 4 BRD4 cooperates with SMAD3 to regulate PAI-1 expression in M2-like TAMs. A WT and *Brd4*-deficient BMDMs were cultured with or without MC38 CM for the indicated times. *Serpine1* mRNA levels were quantified by qRT-PCR. **B** WT and *Brd4*-deficient BMDMs were treated with or without MC38 CM for 24 h. PAI-1 protein levels in the medium were measured by ELISA. **C** PAI-1 protein levels in cell lysates from BMDMs treated as in (**B**) were analyzed by immunoblotting. **D** Tumor samples from WT and *Brd4*- CKO mice, harvested on day 19 post-inoculation, were analyzed for PAI-1 expression by immunoblotting (left), with quantification shown on the right ($n = 5$). **E** BMDMs were pretreated with or without the SMAD3 inhibitor SIS3 (10 μM) for 1 h, then exposed to MC38 CM for 4 h. *Serpine1* mRNA levels were measured by qRT-PCR. **F** BMDMs were pretreated with or without SIS3 (10 μM) for 1 h, followed by MC38 CM treatment for 24 h. Protein levels in cell lysates were assessed by immunoblotting. **G** BMDMs were pretreated with or without SIS3 (10 μM) for 1 h, followed by treatment with or without MC38 CM for 4 h. Endogenous BRD4 was immunoprecipitated, and associated SMAD3 and SMAD4 were detected by immunoblotting. IgG served as a control. **H** Left: Schematic of the murine *Serpine1* promoter region showing the palindrome SMAD binding sequence and two-point mutations (Mu_1 and Mu_2). TSS: transcription start site. Right: pGL3-enhancer reporter plasmids (0.1 μg) containing the wild-type (WT) or mutant *Serpine1* promoter sequences were co-transfected with BRD4 (0.1 μg), SMAD3 (0.05 μg), and SMAD4 (0.05 μg) expression vectors into HEK293T cells. Luciferase activity was measured 48 h post-transfection. **I** *Serpine1* promoter luciferase reporter plasmids (0.1 μg) were co-transfected with SMAD3 (0.05 μg), SMAD4 (0.05 μg), and either wild-type BRD4 or its bromodomain deletion mutant (0.1 μg) into HEK293T cells. Luciferase activity was measured 48 h after transfection. **J** BMDMs were pretreated with or without SIS3 (10 μM, 1 h), followed by MC38 CM treatment for 4 h. Chromatin immunoprecipitation (ChIP) assays were performed using antibodies against BRD4, SMAD3, and RNAPII, and the *Serpine1* promoter was analyzed by qPCR. Results are shown as mean ± SD of three independent experiments. Statistical significance was determined by two-tailed Student's *t* test and one-way ANOVA with multiple comparisons (Tukey test). *$p < 0.05$; **$p < 0.01$; ***$p < 0.005$; ns not significant.

expression dramatically increased luciferase activity (Fig. 4H), indicating that BRD4 facilitates SMAD3/SMAD4-mediated activation of the *Serpine1* promoter. Mutation of critical nucleotides in the SMAD binding sequence [35] significantly diminished SMADs and BRD4's ability to activate the reporter (Fig. 4H), confirming their reliance on this binding site. Moreover, the co-activation by BRD4 appeared bromodomain-dependent, as a bromodomain deletion mutant of BRD4 could not facilitate SMAD-mediated activation (Fig. 4I).

We then performed chromatin immunoprecipitation (ChIP) assays to assess the functional cooperation between BRD4 and SMAD3 on the *Serpine1* promoter. In MC38 CM-treated BMDMs, SMAD3, BRD4 and RNA polymerase II (RNAPII) were enriched at the SMAD binding site on the *Serpine1* promoter (Fig. 4J). Importantly, pre-treatment with SIS3 reduced this enrichment (Fig. 4J), suggesting a SMAD-dependent recruitment process. Collectively, these results highlight the collaborative role of BRD4 with SMAD3 and SMAD4 in enhancing *Serpine1* transcription in polarized TAMs.

BRD4-regulated PAI-1 in TAMs Confers oxaliplatin resistance in CRC via the JAK2/STAT3 signaling pathway

Having identified the cooperation between BRD4 and SMADs to regulate PAI-1 expression in TAM, we next assessed whether BRD4/SMADs-regulated PAI-1 in TAMs contributes to chemoresistance in CRC. We reconstituted recombinant PAI-1 (rPAI-1) into the CM from polarized *Brd4*-deficient TAMs, which had compromised PAI-1 production (Fig. 4B, C), and evaluated its effect on oxaliplatin cytotoxicity against MC38 cells. Supplementing rPAI-1 reduced oxaliplatin-induced apoptosis, as evidenced by decreased cleaved caspase 3 levels and increased cell viability (Fig. 5A–D). This resistance was observed in both mouse and human CRC cells (Supplementary Fig. S9), indicating that BRD4-dependent PAI-1 from polarized TAMs modulates CRC cell sensitivity to oxaliplatin.

Next, we investigated the role of the urokinase receptor (uPAR), which mediates intracellular signaling upon PAI-1 binding [38]. rPAI-1 enhanced viability in WT MC38 cells, but this effect was absent in uPAR knockdown cells (Fig. 5E). Similarly, CM from polarized wild-type TAMs increased oxaliplatin resistance in wild-type MC38 cells but not in uPAR knockdown cells (Fig. 5F), indicating that BRD4-regulated PAI-1 secreted from TAMs targets cancer cells via uPAR to inhibit apoptosis.

We then explored the mechanism underlying PAI-1-mediated oxaliplatin resistance. PAI-1 is known to modulate cell proliferation and chemoresistance through pathways such as PI3K/AKT, JAK/STAT, p38MAPK, and NF-κB [19, 20, 39]. Inhibition of JAK1/2 and PI3K reduced PAI-1-mediated oxaliplatin resistance (Supplementary Fig. S10). Further analysis revealed that PAI-1 specifically enhanced JAK2 phosphorylation in oxaliplatin-treated MC38 cells, without affecting PI3K or p38MAPK signaling (Fig. 5G, Supplementary Fig. S11). Additionally, PAI-1 activated the JAK2/STAT3 pathway, leading to increased STAT3 phosphorylation, nuclear translocation, and anti-apoptotic gene expression (Fig. 5H, Supplementary Figs. S12–S14). Inhibition of STAT3 with S3I-201 reversed PAI-1-mediated resistance (Supplementary Fig. S15). Notably, CM from wild-type TAMs enhanced JAK2/STAT3 activation in oxaliplatin-treated MC38 cells compared to CM from Brd4-deficient TAMs, and this activation was restored by rPAI-1 supplementation (Fig. 5I, Supplementary Fig. S16). These findings underscore the crucial role of the JAK2/STAT3 signaling axis in PAI-1-mediated oxaliplatin resistance.

To evaluate the in vivo impact of BRD4-regulated PAI-1 on oxaliplatin cytotoxicity, we used Tiplaxtinin (PAI-039), a specific PAI-1 inhibitor [40]. While oxaliplatin or PAI-039 alone modestly reduced tumor size, their combination completely halted tumor growth (Fig. 5J–L). This synergy likely resulted from enhanced apoptosis, as indicated by increased TUNEL-positive cells (Fig. 5M, N) and higher levels of cleaved caspase 3 (Fig. 5O). Additionally, STAT3 activation was reduced in tumors treated with both oxaliplatin and PAI-039 (Fig. 5O). These results further support that PAI-1, potentially derived from TAMs, promotes oxaliplatin resistance by inhibiting apoptosis via the JAK2/STAT3 signaling pathway.

High BRD4 expression in TAMs correlates with elevated PAI-1 levels in chemoresistance CRC patients

To investigate the clinical relevance of BRD4 in TAMs on chemoresistance in CRC, we analyzed BRD4 levels in tissue samples from chemotherapy-sensitive and -resistant patients. Immunofluorescence staining indicated that BRD4 was expressed in nearly all cells, including $CD68^+$ TAMs, with significantly higher levels in TAMs from drug-resistant patients compared to those from drug-sensitive patients (Fig. 6A). This suggests a link between BRD4 expression in TAMs and chemotherapy resistance.

We then assessed PAI-1 levels in the same tissue samples and found higher expression in drug-resistant tumor tissues compared to drug-sensitive ones (Fig. 6B). Notably, PAI-1 expression in tumor tissues positively correlated with BRD4 levels in $CD68^+$ TAMs (Fig. 6C), suggesting that BRD4-regulated PAI-1 expression in TAMs is a major source of PAI-1 in CRC tumors. Single-cell RNA-seq analysis of immune cells in the CRC microenvironment [41] confirmed that *SERPINE1* (PAI-1) is primarily expressed in myeloid cells, including TAMs (Fig. 6D) (https://singlecell.broadinstitute.org/single_cell/study/SCP1162). Moreover, high *SERPINE1* expression was associated with shorter relapse-free survival (RFS) in CRC patients undergoing

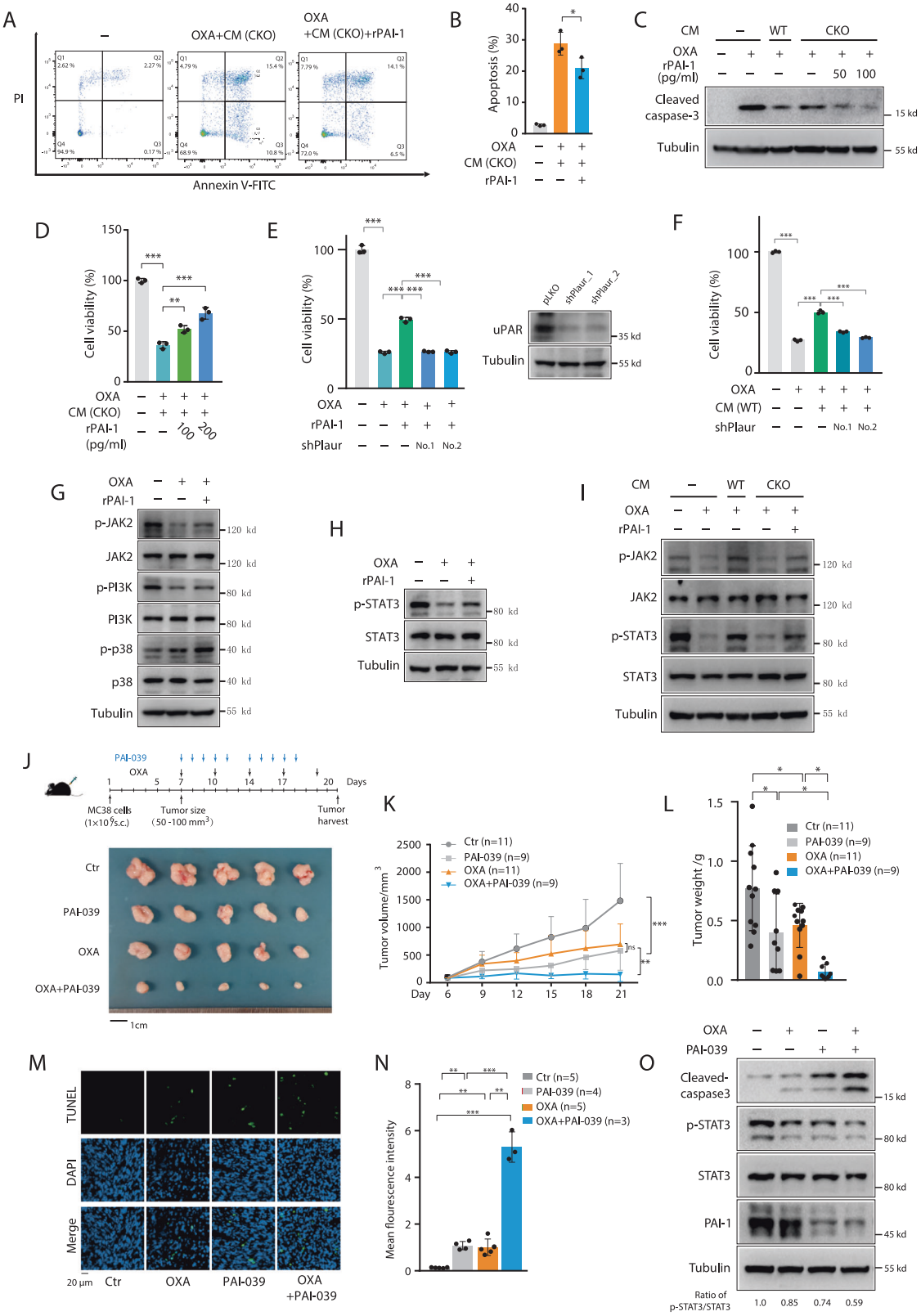

chemotherapy (Fig. 6E). Together, these findings suggest that BRD4-regulated PAI-1 expression in TAMs plays a key role in promoting chemoresistance in CRC. Furthermore, BRD4 levels in TAMs and associated PAI-1 expression in tumors may serve as potential prognostic markers for chemotherapy outcomes in CRC patients.

DISCUSSION

Macrophages play a critical role in innate immunity, defending against pathogens and maintaining tissue homeostasis [42, 43]. They also contribute to the development of various diseases, including metabolic disorders and cancer [44]. Emerging evidence

Fig. 5 BRD4-regulated PAI-1 in TAMs confer MC38 cell resistance to oxaliplatin. A, **B** MC38 cells were cultured with CM from polarized *Brd4*-deficient TAMs, supplemented with or without recombinant PAI-1 (rPAI-1) (100 pg/mL) for 4 h, followed by OXA treatment for 48 h. Apoptotic cells were analyzed by flow cytometry using Annexin V/PI staining. Representative FACS dot plots (**A**) and quantification of apoptotic MC38 cells (**B**) are shown ($n = 3$). **C** MC38 cells were cultured with CM from polarized WT or *Brd4*-deficient TAMs, supplemented with or without rPAI-1 for 4 h, followed by OXA treatment for 8 h. Cleaved-caspase 3 levels in MC38 cells were assessed by immunoblotting. **D** Cell viability of MC38 cells from (**A**) was assessed by MTS assay. **E** MC38 cells transfected with control shRNA or shRNAs targeting *Plaur* were treated with or without rPAI-1 (100 pg/mL), followed by OXA treatment for 48 h. Cell viability was measured by MTS assay, and uPAR/*Plaur* knockdown efficiency is shown on the right. **F** MC38 cells with control or *Plaur* knockdown were treated with CM from polarized WT TAMs for 4 h, followed by OXA treatment for 48 h. Cell viability was assessed by MTS assay. **G**, **H** MC38 cells were incubated with or without rPAI-1 (100 pg/mL) for 4 h, followed by addition of OXA for 8 h. Levels of JAK2, p-JAK2, PI3K, p-PI3K, p38, and p-p38 (**G**), as well as STAT3 and p-STAT3 (**H**), were evaluated by immunoblotting. **I** MC38 cells were exposed to CM from WT or *Brd4*-deficient TAMs, with or without rPAI-1 (100 pg/mL) for 4 h, followed by OXA treatment for 8 h. Levels of JAK2, p-JAK2, STAT3, and p-STAT3 were assessed by immunoblotting. **J** Upper: Experimental schematic. WT mice were subcutaneously inoculated with MC38 cells. On day 7, mice with tumors sized 50–100 mm^3 were intraperitoneally injected with OXA (6 mg/kg body weight) every 3 days, and/or given PAI-039 orally (5 mg/kg body weight) for 5 consecutive days on days 7 and 14. Tumors were harvested on day 21. Representative images of tumors from mice after treatment are shown. Tumor sizes (**K**) and weights (**L**) are presented with the indicated number of mice per group. Representative images (**M**) and quantification (**N**) of TUNEL staining in tumor tissues with the indicated number of animals in each group. **O** Levels of cleaved- caspase 3, STAT3, p-STAT3, and PAI-1 in tumor tissues were analyzed by immunoblotting. Data are shown as mean ± SD. Statistical significance was determined using two-tailed Student's *t* test and one-way ANOVA with Tukey's multiple comparison test. $^{*}p < 0.05$, $^{**}p < 0.01$, $^{***}p < 0.001$.

indicates that BRD4 is a critical regulator of innate immunity and modulates broad biological activities of macrophages [22, 23]. However, its role in the pathological activities of macrophages remains less understood. In current study, we identify a novel pathological function of BRD4 in the polarization of TAMs and the subsequent chemoresistance in CRC. We demonstrate that BRD4 is essential for the polarization of pro-tumor M2-like TAMs and the establishment of immunosuppressive TME. In these polarized M2-like TAMs, BRD4 is recruited to the *Serpine1* promoter via SMAD3/4, driving PAI-1 expression, which in turn promotes chemoresistance through the JAK2/STAT3 signaling pathway in CRC (Fig. 6F). Clinically, elevated BRD4 expression in TAMs of chemotherapy-resistant CRC patients correlates with higher PAI-1 levels (Fig. 6A, C), suggesting that BRD4 and PAI-1 in TAMs may serve as prognostic markers for chemotherapy outcomes.

In vitro and in a syngeneic MC38 mouse model of CRC, BRD4 deficiency in macrophages impaired the polarization of TAMs toward the pro-tumor M2 phenotype (Fig. 1). M2-like TAMs are major contributors to the immunosuppressive TME [30]. In *Brd4*-CKO mice, reduced M2-like TAMs shifted the TME from immunosuppressive to immunostimulatory, characterized by an increase in cytotoxic $CD8^+$ T cells and NK cells, and a decrease in immunosuppressive Tregs and MDSCs (Fig. 1J). This reprogramming of the TME to an immunostimulatory state likely underlies the reduced tumor growth observed in *Brd4*-CKO mice (Figs. 1G and 2A). These findings highlight the potential of targeting BRD4 in TAMs to reshape the TME and improve chemotherapy efficacy in CRC.

In *Brd4*-CKO mice, the proportion of M1-like TAMs was increased, while the proportion of M2-like TAMs was reduced (Fig. 1I). Moreover, the overall number of TAMs was also diminished (Supplementary Fig. S17). This reduction may be attributed to the downregulation of CCR2 expression in TAMs following Brd4 deletion [45] (Supplementary Fig. S18), which likely impairs their recruitment to the tumor site. TAMs play a crucial role in phagocytosing tumor cells, but their activity is often suppressed by "don't eat me" signals presented on the surface of tumor cells, such as the CD47-SIRPα axis [46, 47]. Interestingly, we observed that Brd4 deficiency led to a reduction in *Sirpa* expression in TAMs (Supplementary Fig. S19), which may enhance their phagocytic capacity. Consistent with this, both in vitro and in vivo phagocytosis assays demonstrated that *Brd4*-deficient TAMs exhibited increased ability to engulf tumor cells (Supplementary Figs. S20 and S21). Therefore, the reduced tumor growth observed in *Brd4*-CKO mice appears to result from multiple mechanisms, including enhanced TAM-mediated phagocytosis.

Tumors from *Brd4*-CKO mice demonstrate increased sensitivity to oxaliplatin treatment. After three consecutive low-dose oxaliplatin injections, the tumor sizes in WT mice were reduced by 30%, whereas in *Brd4*-CKO mice, the reduction was more pronounced, reaching 50% (Fig. 2A, B). These results suggest that the knockout of BRD4 in myeloid cells enhances tumor suppression in synergy with oxaliplatin treatment. It is also noteworthy that Brd4 deficiency extends beyond TAMs, as *Brd4*-CKO mice exhibit a lack of BRD4 in other myeloid-derived cells, such as dendritic cells and neutrophils. These additional immune alterations could contribute to the observed anti-tumor phenotype and enhanced chemotherapeutic sensitivity, further underscoring the complex role of BRD4 in regulating the tumor microenvironment. The interplay between Brd4 and different myeloid populations may provide new insights into therapeutic strategies targeting the tumor immune landscape.

Tumors from *Brd4*-deficient mice showed increased sensitivity to oxaliplatin-induced apoptosis, which was associated with changes in the TME (Fig. 2). RNA-seq and cytokine array analysis revealed PAI-1 as a key BRD4-regulated secreted factor in polarized TAMs, contributing to oxaliplatin resistance (Fig. 3). PAI-1 has been implicated in cell proliferation and drug resistance in various cancers, including breast, non-small cell lung, and prostate cancers [14, 16]. In our study, we found that polarized TAMs were the primary source of PAI-1, with its expression regulated by BRD4. While PAI-1 expression was significantly upregulated in WT TAMs by MC38 CM, it remained at basal levels in *Brd4*-deficient TAMs (Fig. 4A–C). Notably, PAI-1 levels were reduced but not abolished in tumors from *Brd4*-CKO mice compared to WT tumors (Fig. 4D). This residual PAI-1 may originate from cancer cells or other TME components, such as endothelial cells and fibroblasts, which also produce PAI-1 [48].

One function of BRD4-regulated PAI-1 from TAMs is its role in conferring resistance to oxaliplatin in colon cancer cells. Supplementing rPAI-1 into CM from polarized *Brd4*-deficient TAMs reduced oxaliplatin-induced apoptosis in cancer cells (Fig. 5A–D). Furthermore, inhibiting PAI-1 with the PAI-1 inhibitor PAI-039 sensitized colon tumors to oxaliplatin-induced apoptosis (Fig. 5J–O). In addition to apoptosis, resistance to oxaliplatin has been linked to other forms of cell death, such as ferroptosis and autophagy [49, 50]. These alternative mechanisms may also contribute to PAI-1-mediated resistance of tumor cells to oxaliplatin. Beyond its paracrine effects on cancer cells, PAI-1 has been shown to promote macrophage recruitment and polarization in cancer [19]. This could potentially establish a positive feedback loop, whereby PAI-1 not only protects tumor cells from chemotherapy but also contributes to the recruitment

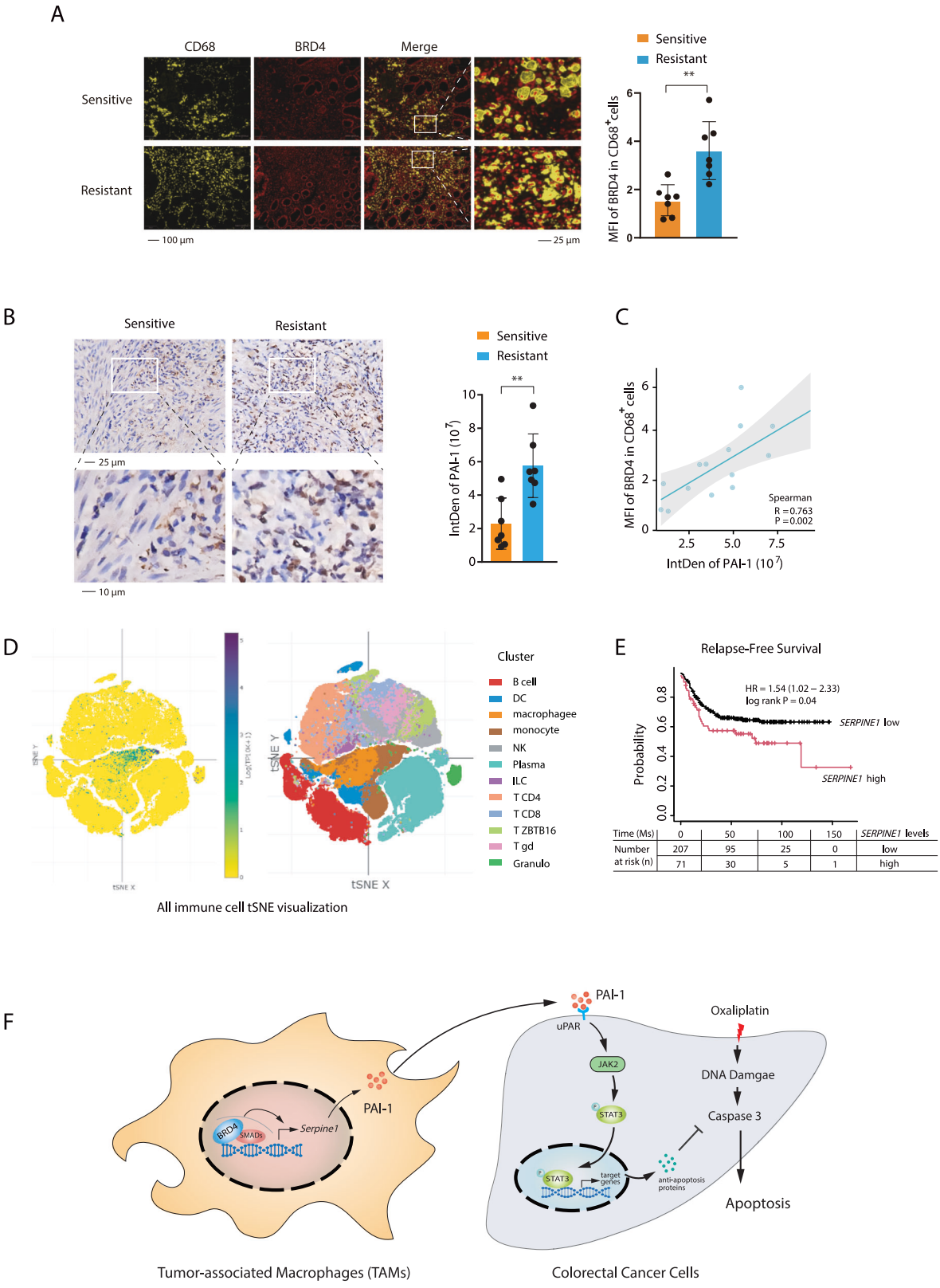

of immune cells that may further facilitate tumor progression. Thus, PAI-1 regulates chemoresistance in cancer cells through both paracrine and autocrine signaling.

SMAD family proteins are key transcription factors regulating PAI-1 expression [17]. Upon stimulation, SMAD3 is phosphorylated, dimerizes with SMAD4, and translocates to the nucleus, where it binds to the SMAD response elements in the PAI-1 (*Serpine1*) promoter to activate transcription [37, 51]. The promoters of human and mouse *Serpine1* share highly homologous sequences, containing response elements for TGF-β, TNF-α, and angiotensin II [52]. A

Fig. 6 BRD4 levels in TAMs correlate with PAI-1 expression in tumor tissues of chemoresistant CRC patients. A Multiplex immunofluorescence images (left panel) and corresponding statistical analysis (right panel) of CD68 (yellow) and BRD4 (red) staining in tumor tissue samples from drug-sensitive ($n = 7$) and -resistant ($n = 7$) CRC patients. **B** Immunohistochemistry images (left panel) and corresponding statistical analysis (right panel) of PAI-1 (brown) staining in tumor tissue samples from drug-sensitive ($n = 7$) and -resistant ($n = 7$) CRC patients. **C** Correlation of protein levels of BRD4 in TAMs ($CD68^+$) and PAI-1 (in total cells) from human CRC tissue samples ($n = 14$). **D** *SERPINE1* expression in immune cells of colon cancer was analyzed in sc-Sequencing datasets (GSE178341). **E** Prognostic significance of *SERPINE1* expression assessed via Kaplan–Meier analysis in CRC patients after chemotherapy. Data are shown as mean ± SD. Two-tailed Student's *t* test was used to calculate *p*-values. $^{**}p < 0.01$. **F** Schematic model of BRD4-mediated polarization of TAMs and the associated drug resistance in CRC. BRD4, in cooperation with SMAD3/SMAD4, regulates the transcription of *Serpine1* and the production of PAI-1 in TAMs. Released PAI-1 targets adjacent cancer cells via uPAR to inhibit oxaliplatin-induced caspase 3 activation and cell apoptosis, leading to chemoresistance.

typical palindromic SMAD binding sequence was identified on the *Serpine1* promoter (Fig. 4H). Mutation of key nucleotides in this sequence abolished the synergistic effect of BRD4 and SMAD3/4 on *Serpine1* transcription (Fig. 4H). Although SMADs alone cannot directly recruit the transcriptional machinery to activate RNAPII, they require co-activators such as p300 or chromatin remodelers [51, 53]. In line with this, SMAD3/4 slightly activated the *Serpine1* luciferase reporter, but co-expression with BRD4 significantly enhanced their transcriptional activity (Fig. 4H), indicating that BRD4 is an important co-activator of SMADs. ChIP assays confirmed that BRD4 binds to the *Serpine1* promoter in a SMAD3-dependent manner upon CM stimulation to activate RNAPII (Fig. 4J). P300-mediated acetylation of SMAD3 increases its DNA binding affinity [54], and BRD4 may bind to acetylated SMAD3 via its bromodomains to further enhance transcription [21, 55]. Indeed, deletion of BRD4's bromodomains abolished its co-activation of SMAD3 in the *Serpine1* luciferase assay (Fig. 4I).

BRD4 acts as a co-activator for SMAD3 in regulating PAI-1 expression in polarized M2-like TAMs (Fig. 4). Whether BRD4 similarly co-activates other SMAD3 target genes in TAMs, influencing their function, remains an open question. SMAD3 has been shown to be essential for the polarization of tumor-associated neutrophils in non-small cell lung cancer [56] and for TGF-β-induced PD-1 expression in macrophages [57]. PD-1 expression in TAMs impairs their phagocytosis and tumor immunity, contributing to an immunosuppressive TME [47]. It is possible that BRD4 co-activates other SMAD3 target genes, including PD-1, to modulate TAM polarization, phagocytosis, and the establishment of an immunosuppressive TME.

What factors in tumor-conditioned medium induce SMAD-mediated PAI-1 expression in TAMs? Since SMADs are key transcription factors activated by TGF-β signaling and tumor cells are a major source of TGF-β production [58], TGF-β is a prime candidate for mediating this effect. Indeed, we tested this hypothesis by adding a TGF-β neutralizing antibody to MC38 CM. This treatment resulted in a significant reduction in *Serpine1* expression in TAMs (Supplementary Fig. S22), supporting the involvement of TGF-β in regulating PAI-1 expression. Additionally, while IgG control had no impact on TAM CM-induced oxaliplatin resistance in MC38 cells, the addition of the TGF-β neutralizing antibody abolished this effect (Supplementary Fig. S23). These results suggest that TGF-β plays a crucial role in establishing a positive feedback loop between colorectal cancer cells and TAMs, where TGF-β-induced PAI-1 expression in TAMs promotes chemoresistance, further reinforcing the tumor's microenvironment in favor of tumor progression.

Comparing to oxaliplatin or PAI-039 monotherapy, PAI-039 in combination with oxaliplatin synergistically suppressed the tumor formation in the MC38 syngeneic CRC mouse model (Fig. 5J), suggesting that chemotherapy in combination with PAI-1 inhibitor could achieve better efficacy in CRC treatment. Furthermore, PAI-1 levels in CRC samples were inversible correlated with the relapse-free survival of CRC patients receiving chemotherapy (Fig. 6E), indicating that PAI-1 is not only a prognostic marker in CRC but could also have prognostic value to predict the outcome of chemotherapy.

BRD4, a member of the BET protein family, has been explored as an anti-cancer target in clinical trials [21]. BRD4 is aberrantly expressed in various tumor cells, where it drives the dysregulated transcription of oncogenes like c-MYC, thereby influencing key processes in tumor biology, including proliferation, metastasis, and immune evasion [59]. BET inhibitors, including BRD4 inhibitors, suppress tumor growth by directly targeting oncoproteins in cancer cells [60]. Our study reveals that BRD4 deficiency in TAMs impairs tumor growth (Fig. 1), suggesting that BRD4 in TAMs also contributes to tumor progression. Therefore, the anti-cancer effects of BRD4 inhibitors may arise not only from their direct action on cancer cells but also from their impact on TAMs. Consistent with this, BET inhibitors such as JQ1 and NHWD-870 have been shown to reprogram the TME and inhibit tumor growth by targeting TAMs [61, 62]. Additionally, we found that JQ1 inhibits SMAD3-mediated transcription of *Serpine1* (Supplementary Fig. S24), potentially enhancing oxaliplatin sensitivity by reducing PAI-1 expression in TAMs. Targeting BRD4 in TAMs could thus enhance chemotherapy sensitivity by reprogramming the TME.

The TME plays a critical role in modulating tumor responses to therapies, including chemotherapy, targeted therapy, and immunotherapy [63]. Immunotherapy relies on activating cytotoxic T cells to eliminate cancer cells [64]. In *Brd4*-CKO mice, the increased number of $CD8^+$ T cells and reduced immunosuppressive Tregs and MDSCs indicated a reprogrammed TME, which may improve responses to immunotherapy. Reprogramming TAMs into tumoricidal macrophages presents a promising strategy for novel immunotherapies. Future studies will investigate the efficacy of ICB therapies in tumor-bearing *Brd4*-CKO mice.

In conclusion, our study identifies BRD4 as a novel regulator of M2-like TAM polarization and TME reprogramming in CRC. Depletion of BRD4 in myeloid cells reprograms TAMs to create an anti-tumor microenvironment, thus suppressing tumor formation (Fig. 1). Notably, several potential TAM-targeting therapies currently in clinical trials, such as those targeting CSF-1R, IL-1A, CCR2, and MARCO [65], are regulated by BRD4. Selective inhibition of BRD4 in TAMs may enhance therapy by targeting multiple TAM-related pathways, offering new opportunities for anti-tumor treatments.

MATERIALS AND METHODS

Detailed materials and methods can be found in Supplemental Information.

DATA AVAILABILITY

The data are available from the corresponding author upon request.

REFERENCES

1. Bray F, Laversanne M, Sung H, Ferlay J, Siegel RL, Soerjomataram I, et al. Global cancer statistics 2022: GLOBOCAN estimates of incidence and mortality worldwide for 36 cancers in 185 countries. CA Cancer J Clin. 2024;74:229–63.

2. Johnson D, Chee CE, Wong W, Lam RCT, Tan IBH, Ma BBY. Current advances in targeted therapy for metastatic colorectal cancer - Clinical translation and future directions. Cancer Treat Rev. 2024;125:102700.
3. Sharma P, Goswami S, Raychaudhuri D, Siddiqui BA, Singh P, Nagarajan A, et al. Immune checkpoint therapy-current perspectives and future directions. Cell. 2023;186:1652–69.
4. Smith SM, Wachter K, Burris HA 3rd, Schilsky RL, George DJ, Peterson DE, et al. Clinical cancer advances 2021: ASCO's report on progress against cancer. J Clin Oncol. 2021;39:1165–84.
5. Guo Y, Wang M, Zou Y, Jin L, Zhao Z, Liu Q, et al. Mechanisms of chemotherapeutic resistance and the application of targeted nanoparticles for enhanced chemotherapy in colorectal cancer. J Nanobiotechnol. 2022;20:371.
6. Bayik D, Lathia JD. Cancer stem cell-immune cell crosstalk in tumour progression. Nat Rev Cancer. 2021;21:526–36.
7. Anderson NM, Simon MC. The tumor microenvironment. Curr Biol. 2020;30:R921–R5.
8. Christofides A, Strauss L, Yeo A, Cao C, Charest A, Boussiotis VA. The complex role of tumor-infiltrating macrophages. Nat Immunol. 2022;23:1148–56.
9. Bleriot C, Dunsmore G, Alonso-Curbelo D, Ginhoux F. A temporal perspective for tumor-associated macrophage identities and functions. Cancer cell. 2024;42:747–58.
10. Pathria P, Louis TL, Varner JA. Targeting tumor-associated macrophages in cancer. Trends Immunol. 2019;40:310–27.
11. Mantovani A, Allavena P, Marchesi F, Garlanda C. Macrophages as tools and targets in cancer therapy. Nat Rev Drug Discov. 2022;21:799–820.
12. Wang S, Wang J, Chen Z, Luo J, Guo W, Sun L, et al. Targeting M2-like tumor-associated macrophages is a potential therapeutic approach to overcome antitumor drug resistance. NPJ Precis Oncol. 2024;8:31.
13. Ha H, Oh EY, Lee HB. The role of plasminogen activator inhibitor 1 in renal and cardiovascular diseases. Nat Rev Nephrol. 2009;5:203–11.
14. Placencio VR, DeClerck YA. Plasminogen activator inhibitor-1 in cancer: rationale and insight for future therapeutic testing. Cancer Res. 2015;75:2969–74.
15. Rossi Sebastiano M, Pozzato C, Saliakoura M, Yang Z, Peng RW, Galie M, et al. ACSL3-PAI-1 signaling axis mediates tumor-stroma cross-talk promoting pancreatic cancer progression. Science advances. 2020;6:eabb9200.
16. Wang B, Gu B, Zhang T, Li X, Wang N, Ma C, et al. Good or bad: Paradox of plasminogen activator inhibitor 1 (PAI-1) in digestive system tumors. Cancer Lett. 2023;559:216117.
17. Dennler S, Itoh S, Vivien D, ten Dijke P, Huet S, Gauthier JM. Direct binding of Smad3 and Smad4 to critical TGF beta-inducible elements in the promoter of human plasminogen activator inhibitor-type 1 gene. EMBO J. 1998;17:3091–100.
18. Datta PK, Blake MC, Moses HL. Regulation of plasminogen activator inhibitor-1 expression by transforming growth factor-beta -induced physical and functional interactions between smads and Sp1. J Biol Chem. 2000;275:40014–9.
19. Kubala MH, Punj V, Placencio-Hickok VR, Fang H, Fernandez GE, Sposto R, et al. Plasminogen activator inhibitor-1 promotes the recruitment and polarization of macrophages in cancer. Cell Rep. 2018;25:2177–91.e7.
20. Che Y, Wang J, Li Y, Lu Z, Huang J, Sun S, et al. Cisplatin-activated PAI-1 secretion in the cancer-associated fibroblasts with paracrine effects promoting esophageal squamous cell carcinoma progression and causing chemoresistance. Cell Death Dis. 2018;9:759.
21. Wu SY, Chiang CM. The double bromodomain-containing chromatin adaptor Brd4 and transcriptional regulation. J Biol Chem. 2007;282:13141–5.
22. Bao Y, Wu X, Chen J, Hu X, Zeng F, Cheng J, et al. Brd4 modulates the innate immune response through Mnk2-eIF4E pathway-dependent translational control of IkappaBalpha. Proc Natl Acad Sci USA. 2017;114:E3993–E4001.
23. Dong X, Hu X, Bao Y, Li G, Yang XD, Slauch JM, et al. Brd4 regulates NLRC4 inflammasome activation by facilitating IRF8-mediated transcription of Naips. J Cell Biol. 2021;220:e202005148.
24. Modi N, Chen Y, Dong X, Hu X, Lau GW, Wilson KT, et al. BRD4 regulates glycolysis-dependent Nos2 expression in macrophages upon H pylori infection. Cell Mol Gastroenterol Hepatol. 2024;17:292–308.e1.
25. Colegio OR, Chu NQ, Szabo AL, Chu T, Rhebergen AM, Jairam V, et al. Functional polarization of tumour-associated macrophages by tumour-derived lactic acid. Nature. 2014;513:559–63.
26. Fang X, Wu Y, Qin H, Zhao P, Shan M, Wang F, et al. Protocol for building an in vitro model of M2-like tumor-associated macrophages with lactic acid or conditioned medium from Lewis cells. STAR Protoc. 2024;5:103120.
27. Xiang X, Wang J, Lu D, Xu X. Targeting tumor-associated macrophages to synergize tumor immunotherapy. Sig Transduct Target Ther. 2021;6:75.
28. Cassetta L, Pollard JW. A timeline of tumour-associated macrophage biology. Nat Rev Cancer. 2023;23:238–57.
29. Liu Y, Zhang Q, Xing B, Luo N, Gao R, Yu K, et al. Immune phenotypic linkage between colorectal cancer and liver metastasis. Cancer cell. 2022;40:424–37.e5.
30. de Visser KE, Joyce JA. The evolving tumor microenvironment: From cancer initiation to metastatic outgrowth. Cancer cell. 2023;41:374–403.
31. Tie Y, Tang F, Wei YQ, Wei XW. Immunosuppressive cells in cancer: mechanisms and potential therapeutic targets. J Hematol Oncol. 2022;15:61.
32. Vasan N, Baselga J, Hyman DM. A view on drug resistance in cancer. Nature. 2019;575:299–309.
33. Xie YH, Chen YX, Fang JY. Comprehensive review of targeted therapy for colorectal cancer. Sig Transduct Target Ther. 2020;5:22.
34. Wang D, Lippard SJ. Cellular processing of platinum anticancer drugs. Nat Rev Drug Discov. 2005;4:307–20.
35. Zawel L, Dai JL, Buckhaults P, Zhou S, Kinzler KW, Vogelstein B, et al. Human Smad3 and Smad4 are sequence-specific transcription activators. Mol cell. 1998;1:611–7.
36. Jinnin M, Ihn H, Tamaki K. Characterization of SIS3, a novel specific inhibitor of Smad3, and its effect on transforming growth factor-beta1-induced extracellular matrix expression. Mol Pharm. 2006;69:597–607.
37. Wrighton KH, Lin X, Feng XH. Phospho-control of TGF-beta superfamily signaling. Cell Res. 2009;19:8–20.
38. Smith HW, Marshall CJ. Regulation of cell signalling by uPAR. Nat Rev Mol Cell Biol. 2010;11:23–36.
39. Balsara RD, Ploplis VA. Plasminogen activator inhibitor-1: the double-edged sword in apoptosis. Thrombosis Haemost. 2008;100:1029–36.
40. Gorlatova NV, Cale JM, Elokdah H, Li D, Fan K, Warnock M, et al. Mechanism of inactivation of plasminogen activator inhibitor-1 by a small molecule inhibitor. J Biol Chem. 2007;282:9288–96.
41. Pelka K, Hofree M, Chen JH, Sarkizova S, Pirl JD, Jorgji V, et al. Spatially organized multicellular immune hubs in human colorectal cancer. Cell. 2021;184:4734–52.e20.
42. Mosser DM, Hamidzadeh K, Goncalves R. Macrophages and the maintenance of homeostasis. Cell Mol Immunol. 2021;18:579–87.
43. Lavin Y, Mortha A, Rahman A, Merad M. Regulation of macrophage development and function in peripheral tissues. Nat Rev Immunol. 2015;15:731–44.
44. Park MD, Silvin A, Ginhoux F, Merad M. Macrophages in health and disease. Cell. 2022;185:4259–79.
45. Hu J, Li G, He X, Gao X, Pan D, Dong X, et al. Brd4 modulates metabolic endotoxemia-induced inflammation by regulating colonic macrophage infiltration in high-fat diet-fed mice. Commun Biol. 2024;7:1708.
46. Logtenberg MEW, Scheeren FA, Schumacher TN. The CD47-SIRPalpha immune checkpoint. Immunity. 2020;52:742–52.
47. Gordon SR, Maute RL, Dulken BW, Hutter G, George BM, McCracken MN, et al. PD-1 expression by tumour-associated macrophages inhibits phagocytosis and tumour immunity. Nature. 2017;545:495–9.
48. Zorio E, Gilabert-Estelles J, Espana F, Ramon LA, Cosin R, Estelles A. Fibrinolysis: the key to new pathogenetic mechanisms. Curr Med Chem. 2008;15:923–9.
49. Bai X, Duan T, Shao J, Zhang Y, Xing G, Wang J, et al. CBX3 promotes multidrug resistance by suppressing ferroptosis in colorectal carcinoma via the CUL3/NRF2/GPX2 axis. Oncogene. 2025. https://doi.org/10.1038/s41388-025-03337-9.
50. Kalli M, Mpekris F, Charalambous A, Michael C, Stylianou C, Voutouri C, et al. Mechanical forces inducing oxaliplatin resistance in pancreatic cancer can be targeted by autophagy inhibition. Commun Biol. 2024;7:1581.
51. Schmierer B, Hill CS. TGFbeta-SMAD signal transduction: molecular specificity and functional flexibility. Nat Rev Mol Cell Biol. 2007;8:970–82.
52. Eren M, Painter CA, Gleaves LA, Schoenhard JA, Atkinson JB, Brown NJ, et al. Tissue- and agonist-specific regulation of human and murine plasminogen activator inhibitor-1 promoters in transgenic mice. J Thromb Haemost. 2003;1:2389–96.
53. Ross S, Cheung E, Petrakis TG, Howell M, Kraus WL, Hill CS. Smads orchestrate specific histone modifications and chromatin remodeling to activate transcription. EMBO J. 2006;25:4490–502.
54. Inoue Y, Itoh Y, Abe K, Okamoto T, Daitoku H, Fukamizu A, et al. Smad3 is acetylated by p300/CBP to regulate its transactivation activity. Oncogene. 2007;26:500–8.
55. Hu J, Pan D, Li G, Chen K, Hu X. Regulation of programmed cell death by Brd4. Cell Death Dis. 2022;13:1059.
56. Chung JY, Tang PC, Chan MK, Xue VW, Huang XR, Ng CS, et al. Smad3 is essential for polarization of tumor-associated neutrophils in non-small cell lung carcinoma. Nature Commun. 2023;14:1794.
57. Lei Z, Tang R, Wu Y, Mao C, Xue W, Shen J, et al. TGF-beta1 induces PD-1 expression in macrophages through SMAD3/STAT3 cooperative signaling in chronic inflammation. JCI insight. 2024;9:e165544.
58. Derynck R, Turley SJ, Akhurst RJ. TGFbeta biology in cancer progression and immunotherapy. Nat Rev Clin Oncol. 2021;18:9–34.
59. Donati B, Lorenzini E, Ciarrocchi A. BRD4 and Cancer: going beyond transcriptional regulation. Mol cancer. 2018;17:164.
60. Jung M, Gelato KA, Fernandez-Montalvan A, Siegel S, Haendler B. Targeting BET bromodomains for cancer treatment. Epigenomics. 2015;7:487–501.
61. Yin M, Guo Y, Hu R, Cai WL, Li Y, Pei S, et al. Potent BRD4 inhibitor suppresses cancer cell-macrophage interaction. Nat Commun. 2020;11:1833.

62. Wang H, Tang Y, Fang Y, Zhang M, Wang H, He Z, et al. Reprogramming tumor immune microenvironment (TIME) and metabolism via biomimetic targeting codelivery of shikonin/JQ1. Nano Lett. 2019;19:2935–44.
63. Bejarano L, Jordao MJC, Joyce JA. Therapeutic targeting of the tumor microenvironment. Cancer Discov. 2021;11:933–59.
64. Waldman AD, Fritz JM, Lenardo MJ. A guide to cancer immunotherapy: from T cell basic science to clinical practice. Nat Rev Immunol. 2020;20:651–68.
65. Mantovani A, Marchesi F, Malesci A, Laghi L, Allavena P. Tumour-associated macrophages as treatment targets in oncology. Nat Rev Clin Oncol. 2017;14:399–416.

ACKNOWLEDGEMENTS

We thank Cailing Yan from the Public Technology Service Center at Fujian Medical University for assistance with the IVIS® Spectrum In Vivo Imaging System analysis. This work was supported by the National Natural Science Foundation of China (81902842 to XMH and 81801974 to JFH), the Natural Science Foundation of Fujian Province (2022J01210 to DP, 2020J01615 to JFH and 2021J01669 to XMH), the Joint Funds for Innovation in Science and Technology, Fujian Province (2023Y9001 to XMH and 2020Y9006 to JFH), the Young and Middle-Aged Key Personnel Training Project of the Fujian Provincial Health Commission (2021GGA029 to DP); and the UIUC Research Board (RB24044) and CCIL Seed Grant to LFC.

AUTHOR CONTRIBUTIONS

XMH and LFC designed the experiment; DP, JFH, GL, XMG, JW, LSJ, HL, YLC, YRZ and YHC performed the experiments; XMH, DP, JFH, GL, JW, XMG, LSJ, HL, YLC, YHC, YRZ, JJL, MZ, HC, and LFC analyzed the data; XMH, LFC and HC supervised the research; DP, XMH and LFC wrote the manuscript.

COMPETING INTERESTS

The authors declare no competing interests.

ETHICS APPROVAL

All human tissue investigations in this study were conducted in accordance with protocols approved by the Ethics Committee of the First Affiliated Hospital of Fujian Medical University (MRCTA, ECFAH of FMU 2021-423). Informed consent was obtained from all patients prior to the use of tumor tissues and clinical data. All animal experiments were approved by the Institutional Animal Care and Use Committee of Fujian Medical University (IACUC FJMU 2023-Y-0652).

ADDITIONAL INFORMATION

Supplementary information The online version contains supplementary material available at https://doi.org/10.1038/s41388-025-03453-6.

Correspondence and requests for materials should be addressed to Hui Chen, Lin-Feng Chen or Xiangming Hu.